# Role of the Interfacial Orientation in Adhesion between Semicrystalline Polymers

**ARTICLE** *in* MACROMOLECULES · APRIL 2001

Impact Factor: 5.8 · DOI: 10.1021/ma0017790

# Role of the Interfacial Orientation in Adhesion between Semicrystalline Polymers

**C. Laurens,*,† R. Ober,† C. Creton,‡ and L. Léger*,†**

*Laboratoire de Physique de la Matière Condensée, Collège de France, 11 place Marcelin Berthelot, 75231 Paris, Cedex 05, France, and Laboratoire de Physico-Chimie Structurale et Macromoléculaire, ESPCI, 10 rue Vauquelin, 75231 Paris, Cedex 05, France*

*Received October 13, 2000; Revised Manuscript Received February 20, 2001*

ABSTRACT: To understand the molecular mechanisms responsible for the adhesion between isotactic polypropylene (iPP) and polyamide 6 (PA6) in the presence of iPP−PA6 diblock copolymer, thin film assemblies with a typical thickness of 115 nm have been prepared. The crystalline orientation of the iPP and of the PA6 close to the interface has been investigated by X-ray diffraction. An epitaxial crystallization of iPP on PA6 was observed. Similarly to what happens for adhesive strength, the epitaxy is enhanced when increasing the copolymer surface density or the length of the PP block and further enhanced when the samples were annealed above the melting temperature of PA6.

## Introduction

Most polymer pairs are immiscible and present a mechanically weak interface due to the lack of entanglements between the two types of chains. A compatibilizing component is then generally added to polymer blends to prevent interfacial failure between the two phases. This additive, for instance a diblock copolymer, acts as a molecular connector entangled with chains on both sides of the interface.[1−3] Its presence decreases the interfacial tension between the two polymers, stabilizing a finely dispersed morphology in the blend, and increases the mechanical strength of the interface. We will focus here on the mechanical role of the compatibilizer only.

While the molecular characteristics for effective reinforcement are well-known for glassy polymers,[4,5] the situation is less clear for semicrystalline polymers. A useful model for this case is the interface between isotactic polypropylene (iPP) and polyamide 6 (PA6), both semicrystalline polymers. This interface is reinforced with an iPP−PA6 diblock copolymer formed in situ by chemical reaction between the $-NH_2$ end of polyamide chains and modified polypropylene chains bearing succinic anhydride groups. Previous studies[6,7] showed that in most experimental conditions the influence of connecting chains on the fracture toughness of such assemblies is similar to what is observed for assemblies of glassy polymers: for long enough copolymers, the applied stress is sufficient to activate bulk plastic deformation and $G_c \sim \Sigma^2$ where $G_c$ is the critical energy release rate and $\Sigma$ the surface density of copolymer at the interface.[8] Yet, a strong increase of the efficiency of copolymer molecules in enhancing the fracture toughness was observed for specific experimental conditions, namely, when the system containing copolymers with a "long" iPP block was annealed above the melting temperature of PA6.

This enhanced efficiency was not observed for assemblies between glassy polymers and is then presumably related to the semicrystalline nature of the polymers. Boucher[7] suggested that this phenomenon could be related to the presence of the $\beta$-phase of iPP near the interface of the samples, but subsequent experiments invalidated that hypothesis.[9] The microstructure near the interface was also studied by transmission electron microscopy:[9,10] the authors did not notice differences in that microstructure between samples annealed above or below the PA6 melting temperature. The fact that neither a modification of the crystal structure in the bulk iPP phase nor a change of the microstructure near the interface can explain this increase in fracture toughness strongly suggests that the crystalline structure in the *immediate* vicinity of the interface plays a role in this strengthening effect, maybe through the coupling, in the same crystallite, between the iPP chains and the iPP−PA6 block copolymer.

Grazing angle X-ray scattering appears as a good tool to study this coupling between semicrystalline polymers at molecular scales. The roughness of the interface in assemblies used for the adhesion measurements limits however the resolution of this method. To overcome that difficulty, we prepared thin films bilayers on silicon wafers. The crystalline orientation at the interface has been investigated by X-ray diffraction experiments. The influence of the presence of copolymer and of the annealing time and temperature will be discussed, in relation with the behavior of macroscopic samples.

## Experimental Section

**Materials and Sample Preparation.** The polyamide 6 was Ultramid B3 from BASF ($M_n \cong 13$ kg/mol, $M_w/M_n = 2$, $T_m = 223$ °C), with an average of one $-NH_2$ end per chain. Isotactic polypropylene 3050MN1 from APPRYL ($M_n \cong 57$ kg/mol, $M_w/M_n = 4.8$, $T_m = 165$ °C) mixed with 5 wt % of succinic anhydride functionalized PP ($PP_f$) was used for the other part of the assemblies. Such blends will be denoted PP* in the following. Two $PP_f$ synthesized by Elf Atochem, having one average anhydride per chain, were used ("short chains", $M_n \cong 25$ kg/mol, and "long chains", $M_n \cong 40$ kg/mol).

Thin film bilayers were prepared by spin-coating solutions onto silicon wafers (Siltronix). The wafers were cleaned by the UV/ozone method[11] for 1 h before being used. Some of them were grafted with (3-aminopropyl)triethoxysilane (APS) so that their surface presented amino groups which could react with

† Collège de France.
‡ ESPCI.
* To whom correspondence should be addressed. E-mail claire.laurens@college-de-france.fr or lleger@ext.jussieu.fr.

10.1021/ma0017790 CCC: $20.00 
Published on Web 03/28/2001

the $PP_f$ chains: 10 drops of APS (Fluka, purity 96%) were poured in 10 mL of dry toluene (SDS, purity ≥ 99.3%). The wafer was kept 15 min in the solution, washed with toluene and ethanol, dried at 90 °C for 15 min, and subsequently washed with toluene and ethanol.

PA6 films were deposited by spin-coating on bare silicon wafers from solutions (0.83 wt % PA6) in pure formic acid (R.P. Rectapur, purity ≥ 98%) at room temperature. They were subsequently dried for 1 h at 80 °C under vacuum. Solutions of iPP (0.83 wt % PP) were prepared in hot xylene (R.P. Normapur, mixture of isomers) at $T \cong 130$ °C under argon to avoid the oxidation of the polymer. PP films were then deposited on hot surfaces (bare silicon wafers, APS-grafted wafers or PA6 films on silicon) to prevent the polymer precipitation. In all cases the rotation speed of the wafer was 2500 rpm.

The thin films were annealed under vacuum to avoid the oxidation of PP. The wafers were placed on a hot surface (140 °C), and the system was heated above the melting temperature of iPP. Annealing temperatures were varied from 180 to 223 °C and annealing times from 30 to 120 min. Note that we called "annealing time" the time during which the temperature was greater than the melting temperature of iPP (i.e., 165 °C) and that the time during which the temperature was constant was sensibly smaller. The samples were then cooled to 125 °C (cooling rate ≅ 1 °C/min) and quenched at room temperature.

**Sample Characterization.** Film thickness was measured by ellipsometry with a Sentech ellipsometer ($\lambda = 632.8$ nm).

Photographs of the samples were taken with a Reichert-Jung Polyvar MET microscope in the reflection mode.

The X-ray generator used in the diffraction experiments (Rigaku RU-200BEH) is a rotating anode operating at 40 kV and 25 mA with a copper target. A germanium (111) monochromator is used to select the Cu $K\alpha_1$ line ($\lambda = 0.154\,05$ nm). The experiments were performed in the reflection mode with various incidence angles between $\alpha = 0.5°$ (low incidence) and $\alpha = 9°$ ($\theta/2\theta$ configuration, which allows the observation of the planes parallel to the surface).

In most cases the reflected beam is detected by a linear detector at a distance of 19.9 cm from the sample. The detector is placed at $2\theta = 18°$ to detect the main diffraction peaks of the polymers. The spectra were scaled in time in order to correspond to an exposition time of 1000 s. A few spectra were recorded with a 2D detector (Photonic Science), placed at 18.2 cm from the sample, and centered in the position $2\theta = 18°$.

## Results and Discussion

**Samples Morphology.** Film thickness were systematically measured before annealing; they were about 55 nm (±5%) for PA6 films and 60 nm (±10%) for PP films. Thickness were calculated as the average of at least 10 measurements on each film surface.

Observation of the annealed samples clearly showed the effectiveness of the iPP−PA6 copolymer as a compatibilizing agent for our assemblies. Samples of pure iPP matrix deposited on PA6 presented holes due to the dewetting of iPP even for low annealing temperatures and short annealing times (Figure 1a), while no dewetting was observed for samples containing $PP_f$ (Figure 1b), whatever the annealing times and temperatures tested. Such observations strongly suggest that the chemical grafting of $PP_f$ on the PA6 surface took place and that the presence of iPP−PA6 copolymer at the interface prevents the dewetting of the iPP matrix on the PA6 substrate.

Great differences in the iPP crystallites morphology were observed between iPP films deposited on bare or grafted silicon wafers and films deposited on PA6 surfaces as illustrated in Figure 2: in the last case, the crystallites are smaller and lose the 2D spherulitic

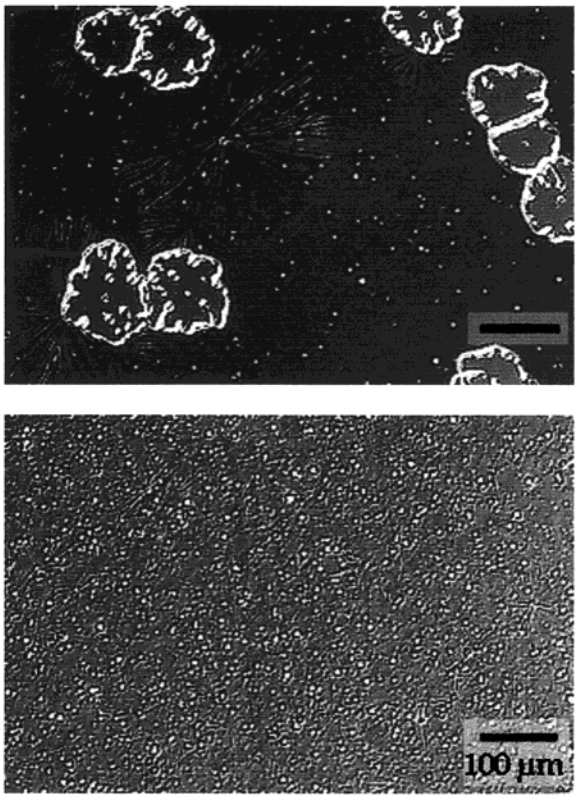


**Figure 1.** Photographs of PP films deposited on PA6 and annealed at 182 °C: (a, top) film of pure PP matrix, annealed for 45 min; (b, bottom) film of PP matrix mixed with 5 wt % $PP_f$ (PP*), annealed for 100 min.

shape observed on silicon wafers. These observations suggest an influence of the substrate on iPP crystallization.

**Crystalline Orientation at the Interface.** A crystalline orientation can be detected in a polymer film by X-ray diffraction since the diffracted intensity depends on the incidence angle. The intensity diffracted by ($hkl$) planes in a thickness "d$x$" at a depth "$x$" of an isotropic sample is given by eq 1:[12]

$$\mathrm{d}I_{hkl} = i_{hkl} p_{hkl} S \frac{\mathrm{d}x}{\sin\alpha} \exp\left[-2\mu\rho x\left(\frac{1}{\sin\alpha} + \frac{1}{\sin(2\theta - \alpha)}\right)\right] \quad (1)$$

with $i_{hkl}$ the intensity diffracted by one crystallite, $p_{hkl}$ the probability for ($hkl$) planes to be in diffraction position, $S$ the cross section of the beam, $\mu$ the mass absorption coefficient of the material, $\rho$ its density, $\theta$ the Bragg's angle, and $\alpha$ the incidence angle. For a film thickness $e$ of about 100 nm, $\exp\{-2\mu\rho e[(\sin\alpha)^{-1} + (\sin(2\theta - \alpha)^{-1}]\} \approx 1$ and $I_{hkl}$ is related to $e$ and $\alpha$ by eq 2:

$$I_{hkl} \approx i_{hkl} p_{hkl} S \frac{e}{\sin\alpha} \quad (2)$$

Thus, the intensity diffracted by an isotropic polymer thin film decreases when $\alpha$ increases. Because of the small quantity of material present in the sample, only the most intense diffraction peaks should be observable. On the other hand, if a film is oriented so that ($hkl$) planes are parallel to the film surface, $p_{hkl}$ is high for $\alpha \approx \theta$, and the intensity diffracted by these planes is not

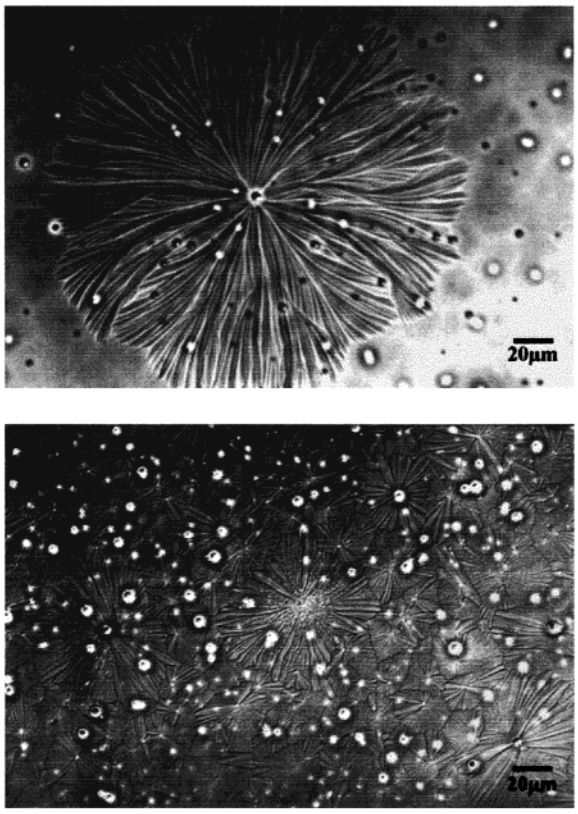


**Figure 2.** Photographs of PP* films deposited on different substrates and annealed at 180 °C. (a, top) Film deposited on bare silicon wafer (annealing time: 50 min). Large spherulites (diameter about 200 $\mu$m) grew in the two dimensions of the film. Crystallites grown on APS grafted silicon wafers have the same morphology. (b, bottom) Film deposited on a PA6 film (annealing time 30 min). The crystallites are smaller (typically 20 $\mu$m) and have a completely different shape.

expected to decrease so quickly with α. A signal should then be detectable in the $\theta/2\theta$ configuration.

Figure 3 shows 2D diffraction spectra obtained for polypropylene on different substrates: bulk iPP α-phase (reference, Figure 3a), PP* film on silicon wafers (Figure 3b), and PP* film on a PA6 film (Figure 3c). All the diffraction rings characteristic of the isotropic iPP α-phase are visible in Figure 3a. In the case of PP* films deposited on bare silicon wafers, only the most intense diffraction ring of bulk iPP was detectable for a low incidence angle ($\alpha = 0.5°$), and no intensity was detected for larger α. Such an evolution of the diffracted intensity with α is characteristic of nonoriented films as discussed above. Note that the spectra obtained for PP* on APS grafted silicon wafers are similar to those obtained on bare silicon wafers. These results show clearly that PP* films on silicon wafers are nonoriented and that the grafting of $PP_f$ on the substrate does not induce any specific orientation of the iPP. The spectra of PP* films deposited on PA6 are completely different. An intense diffraction peak is observed for the (040) planes whatever the incidence angle (between 0.5° and 9°), which indicates an oriented sample, with (040) planes parallel to the interface. Besides, only a little part of the diffraction ring is visible for $\alpha = 9°$ (Figure 3c), which confirms that the PP part of these assemblies is quite well oriented. This demonstrates that PA6 induces a specific orientation of the polypropylene phase so that $(040)_{PP}$ planes are parallel to the film surface.

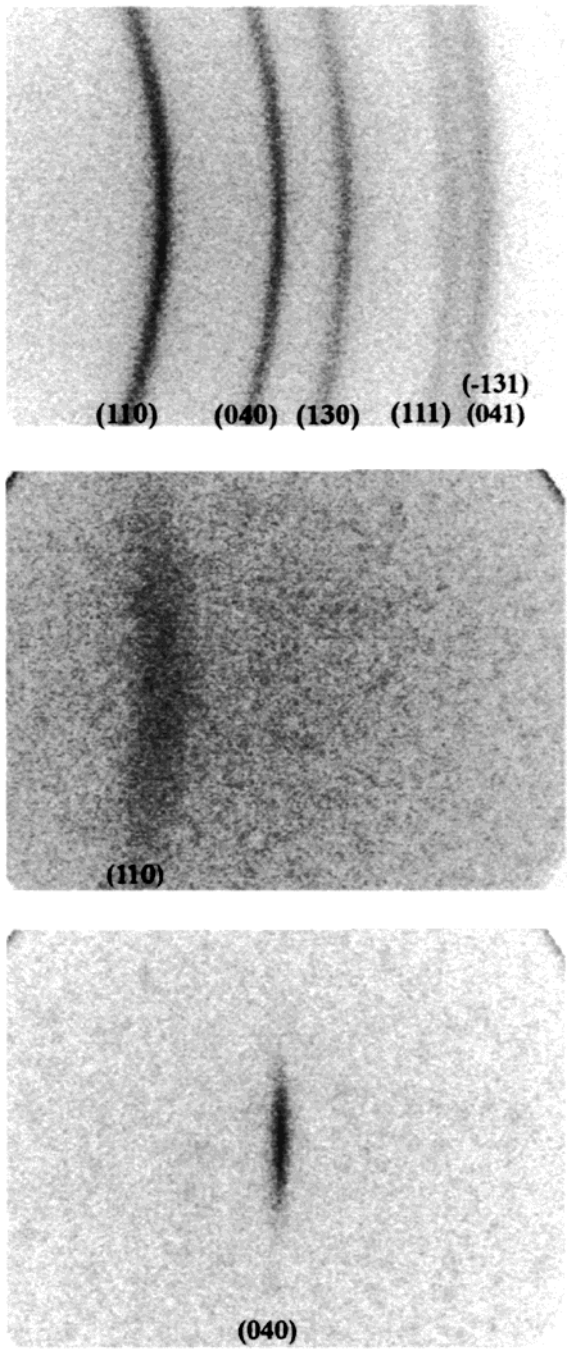


**Figure 3.** 2D diffraction spectra of isotactic polypropylene on different substrates. (a, top) Bulk iPP (part of an extruded sheet used as received). Spectrum acquired in transmission mode (acquisition time: 3 h 30). Note that all the diffraction rings of isotropic iPP α-phase are visible. (b, middle) PP* film deposited on a silicon wafer and annealed 83 min at 200 °C. Spectrum acquired in the reflection mode with an incidence angle $\alpha = 0.5°$ and an exposition time of 15 h. The only perceptible diffraction ring corresponds to (110) planes. (c, bottom) PP* film deposited on a PA6 film and annealed 85 min at 200 °C. Spectrum acquired in the reflection mode with an incidence angle $\alpha = 9°$ (exposition time: 10 h). The only visible diffraction ring corresponds to (040) planes. Note that only a part of the ring is present, which indicates a good orientation of the polymer with (040) planes parallel to the interface.

In the following we will present and discuss data showing how the annealing conditions influence the observed orientation. All data presented in Figures 4−6 have been recorded with the linear detector and scaled

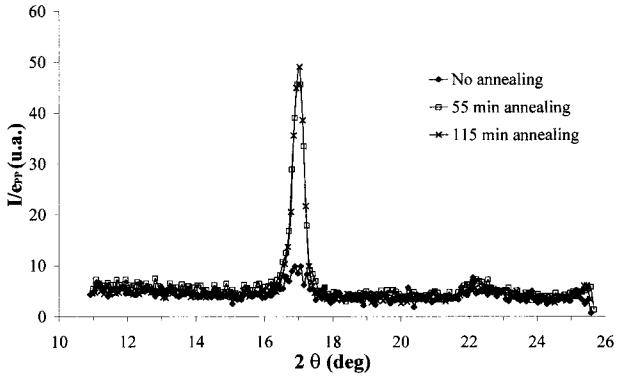


**Figure 4.** Influence of the annealing time on PP crystalline orientation. Films of PP* containing "long" $PP_f$ chains deposited on PA6 films. Samples annealed at 200 °C.

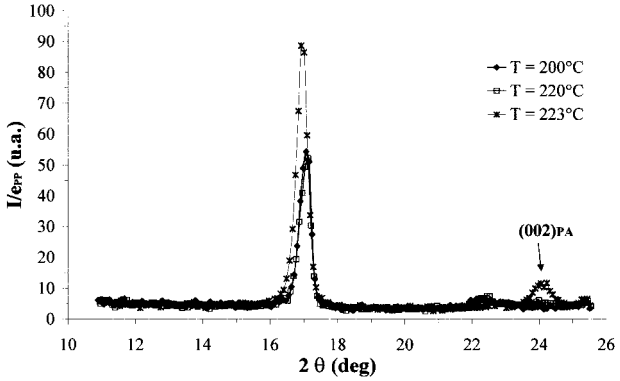


**Figure 5.** Influence of the annealing temperature on PP and PA6 crystalline orientation. Films of PP* containing "long" $PP_f$ chains deposited on PA6 films. Samples annealed 90 min.

in time to be qualitatively and quantitatively compared; the incidence angle was $\alpha = 9°$ so that we observed the planes parallel to the interface. We divided the diffracted intensities by the PP film thickness (measured before annealing): as shown in eq 2, $I_{hkl}$ depends on the film thickness, and $I/e_{PP}$ is a good parameter to quantify the orientation in the iPP films.

As shown in Figure 4, increasing the annealing time led to an enhanced diffracted intensity by $(040)_{PP}$ planes, i.e., to an enhanced iPP orientation. In Figure 5, the effect of increasing the annealing temperature to 223 °C (the melting temperature of PA6) is reported. A reorganization of both phases is observed. The PA6 organizes with the (002) planes parallel to the film surface upon melting ($2\theta_{(002)} = 24.0°$). Simultaneously, the iPP orientation appears to be much greater than for lower annealing temperatures. The length of the copolymer PP block also appears to influence the epitaxy: a slight difference exists between the diffraction spectra obtained with assemblies containing "short" and "long" $PP_f$ chains, the diffracted intensity being a little higher in the last case, especially for high annealing temperatures, as shown in Figure 6.

## Discussion

This set of experiments reveals an epitaxial crystallization of isotactic polypropylene on the polyamide 6 substrate: $(010)_{PP}$ and $(001)_{PA6}$ planes (polymer chains planes[23]) tend to be parallel to each other. This may seem surprising as, in our samples, PA6 crystallizes on spin-coating and is not preoriented. Nevertheless, even in a nonoriented sample, a certain amount of lamellae are oriented so that they can induce the epitaxy of iPP.

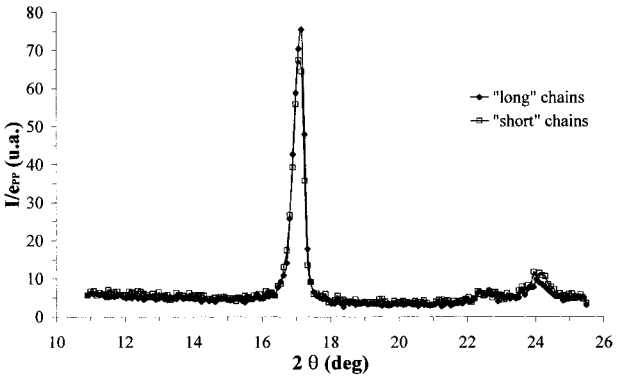


**Figure 6.** Influence of the PP block length of the copolymer on PP orientation. Films of PP* containing respectively "long" and "short" $PP_f$ chains deposited on PA6 films. Samples annealed simultaneously at 223 °C for 75 min.

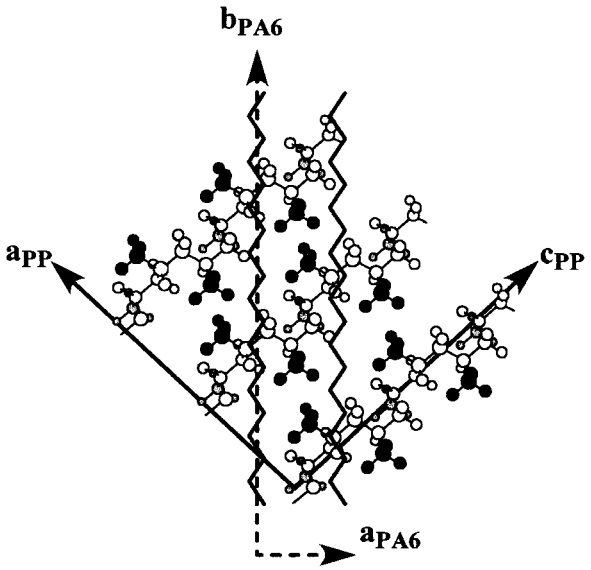


**Figure 7.** Schematic representation of the relative positions and orientations of PA6 ((001) plane) and iPP chains ((010) plane) for left-handed iPP helix. The PA6 chains and the rows of methyl groups are vertical and make an angle of 50° with the iPP chain axis. A relatively good matching exists between the distance between two methyl rows (0.505 nm) and the interchain distance in $(002)_{PA6}$ planes (0.478 nm).

This orientation can then propagate in the iPP phase even if the PA6 does not melt during the annealing. That epitaxy between iPP and PA6 can be related to previous results on the epitaxial crystallization of the helical chains of isotactic polypropylene on aliphatic polymers with a planar zigzag conformation such as polyethylene, polyamides, polyesters, etc.[15−17] The epitaxial orientation is interpreted as shown in Figure 7 as the result of the parallel alignment of the aliphatic (zigzag) chains with rows of iPP methyl groups, leading to a disposition of the polymers with their chain axis tilted at 50° to each other.[15] In our system, the formation of iPP/PA6 copolymer during the annealing allows the observation of the epitaxy by preventing the dewetting of iPP from the PA6 surface. Note that a consequence of the observed orientation is that if a copolymer chain crystallizes on both sides of the interface, it will be, at least locally, *parallel* to the interface and not orthogonal as in the usual representation.

The tendency of iPP to orient on PA6 exists whatever the annealing conditions and the $PP_f$ used, but these conditions and the presence of copolymer strongly

influence the degree of orientation. As seen in Figure 3, a longer annealing time leads to a more effective orientation. As previously shown,[6,7] increasing the annealing time increases Σ, the surface density of copolymer at the interface: the formation of iPP/PA6 copolymer chains stabilizes the interface and favors the existence of the interfacial orientation. The length of the copolymer PP block also appears to influence the epitaxy: the orientation is slightly more pronounced when the PP block of the copolymer is long, especially for high annealing temperatures. Finally, we have observed that the epitaxy is clearly more effective above the melting temperature of PA6, with a reorganization of both iPP and PA6 phases. The PA6 film recrystallized with (001) planes parallel to the interface, an orientation that we also observed for a thin PA6 film deposited on a silicon wafer without iPP on top of it and annealed above 223 °C. Muratoglu et al.[18] showed that PA6 films deposited on rubber surfaces and remelted developed the same crystalline orientation, with the low-energy (001) planes parallel to the interface. The iPP surface is then not directly responsible for the observed PA6 reorientation but, being of low energy, could favor it. Once the PA6 is reoriented, the number of PA6 lamellae able to induce the iPP epitaxy is larger and the iPP orientation is greater, as shown in Figure 5.

These results show that the degree of epitaxy of iPP on PA6 is influenced by the same factors as the fracture toughness of macroscopic assemblies. First, an enhanced orientation is observed when Σ is increased. Second, annealing conditions close to those that lead to enhanced fracture toughness in the macroscopic samples (i.e., $T \cong T_m$(PA6) and copolymer with a "long" PP block) cause an enhanced epitaxy in the films. The two effects could be correlated. Such correlations between the occurrence of epitaxy and improved mechanical properties have already been suggested. For instance, a relation has been suggested between improved macroscopic adhesion and the presence of epitaxy in the case of a PP copolymer matrix toughened with EPR particles.[19] Epitaxial crystallization has also been shown to improve the mechanical properties of isotactic polypropylene/polyethylene or isotactic polypropylene/polybutadiene assemblies.[17,20−22] The authors explain this improvement by the fact that the epitaxially recrystallized lamellae can bridge the soft amorphous regions in the substrate lamellar structure. At the present time, we are not able to present a detailed model explaining the role of epitaxy in the enhanced coupling efficiency of the long iPP block copolymer molecules at high temperatures. We suspect that copolymer chains crystallized on both faces of the interface probably play a role in this mechanism. Experiments with other copolymer molecules unable to cocrystallize with iPP are presently underway to try to understand the exact role of a possible cocrystallization of the copolymer in both epitaxy and enhanced adhesion.

## Conclusion

Our experiments on thin films modeling the iPP/PA6 interface have clearly shown an epitaxial crystallization of isotactic polypropylene on polyamide 6. This epitaxy is influenced by the same factors as the fracture toughness of the interface on macroscopic samples, namely the surface density of a iPP−PA6 copolymer, the length of the iPP block of this copolymer and the annealing temperature.

Some additional experiments must be made to correlate more precisely the behavior of the thin films investigated in the present study and of the macroscopic samples used in fracture toughness measurements. In particular, we shall compare the surface density of copolymer at the interface in both types of samples annealed in identical conditions. To further elucidate the role of the copolymer in the epitaxy, experiments varying the tacticity of the $PP_f$ block and its ability to crystallize in the same lamellae as the iPP matrix are presently underway.

**Acknowledgment.** The authors thank Atofina for its financial support and for providing the materials.

## References and Notes

(1) Fayt, R.; Jérôme, R.; Teyssié, P. *J. Polym. Sci., Part B: Polym. Phys.* **1989**, *27*, 775−793.
(2) Brown, H. R. *Macromolecules* **1989**, *22*, 2859−2860.
(3) Creton, C.; Kramer, E. J.; Hadziioannou, G. *Macromolecules* **1991**, *24*, 1846−1853.
(4) Kramer, E. J.; Norton, L. J.; Dai, C.-A.; Sha, Y.; Hui, C. Y. *Faraday Discuss.* **1994**, *98*.
(5) Creton, C. In *Polymer Surfaces and Interfaces III*; Richards, R. W., Pearce, S. K., Eds.; John Wiley & Son Ltd: New York, 1999; pp 101−147.
(6) Boucher, E.; Folkers, J. P.; Hervet, H.; Léger, L.; Creton, C. *Macromolecules* **1996**, *29*, 774−782.
(7) Boucher, E.; Folkers, J. P.; Creton, C.; Hervet, H.; Léger, L. *Macromolecules* **1997**, *30*, 2102−2109.
(8) Brown, H. R. *Macromolecules* **1991**, *24*, 2752−2756.
(9) Kalb, F. Ph.D. Thesis, Université Paris VI-Pierre et Marie Curie, 1998.
(10) Plummer, J. G.; Kausch, H.-H.; Creton, C.; Kalb, F.; Léger, L. *Macromolecules* **1998**, *31*, 6164−6176.
(11) Vig, J. R. In *Treatise on Clean Surfaces Technology*; Mittal, K. L., Ed.; Plenum Press: New York, 1987; p 1.
(12) Guinier, A. *Théorie et technique de la radiocristallographie;* Dunod: Paris, 1964.
(13) Natta, G.; Coradini, P. *Del Nuevo Cimento* **1960**, *15*, 40−51.
(14) Holmes, D. R.; Bunn, C. W.; Smith, D. J. *J. Polym. Sci.* **1955**, *17*, 139−177.
(15) Lotz, B.; Wittmann, J. C. *J. Polym. Sci., Part B: Polym. Phys.* **1986**, *24*, 1559−1575.
(16) Wittmann, J. C.; Lotz, B. *Prog. Polym. Sci.* **1990**, *15*, 909−948.
(17) Petermann, J. In *Polypropylene: Structure, Blends and Composites;* Karger-Kocsis, J., Ed.; Chapman & Hall: London, 1995; Vol. 1, pp 140−164.
(18) Muratoglu, O. K.; Argon, A. S.; Cohen, R. E. *Polymer* **1995**, *36*, 2143−2152.
(19) Kestenbach, H.-J.; Loos, J.; Petermann, J. *Polym. Eng. Sci.* **1998**, *38*, 478−484.
(20) Gross, B.; Petermann, J. *J. Mater. Sci.* **1984**, *19*, 105−112.
(21) Petermann, J.; Xu, Y. *Colloids Polym. Sci.* **1991**, *269*, 455−459.
(22) Lee, H.; Schultz, J. M. *J. Mater. Sci.* **1988**, *23*, 4237−4243.
(23) PP chain axis is **c**[13] (as usual for polymers), but PA6 chain axis is **b** for historical reasons.[14]

MA0017790